JOURNAL OF Materials CHEMISTRY

Template-based synthesis of nanoscale Ag_2E (E = S, Se) dendrites

Jianping Xiao, Yi Xie,* Rui Tang and Wei Luo

Structure Research Laboratory, and Lab of Nanochemistry & Nanomaterials, University of Science and Technology of China, Hefei, Anhui, 230026, P. R. China.
E-mail: yxie@ustc.edu.cn; Fax: 86-551-3603987; Tel: 86-551-3603987

Received 9th November 2001, Accepted 23rd January 2002
First published as an Advance Article on the web 25th February 2002

Herein, well-defined nanoscale Ag_2S and Ag_2Se dendrites, which represent a novel morphology of silver chalcogenides, were successfully synthesized using a template-based method at room temperature and ambient pressure. It was found that the template and ultrasonic wave played important roles in the formation of well-defined dendrites. The products were characterized by X-ray diffraction (XRD), transmission electron microscopy (TEM), X-ray photoelectron spectroscopy (XPS) and elemental analysis. The optical properties of the products were also recorded by means of UV-Vis absorption spectroscopy, indicating that the products were within a quantum confinement regime. Finally, the formation mechanism of dendrites was also investigated.

Introduction

Late transition metal chalcogenides have a number of commercial applications in pigments, semiconductors and fluorescence devices.[1] Silver sulfide is a good prospective optoelectronic and thermoelectric material, which is often used as a photosensitizer for photographic purposes.[2] Silver selenide, a well-known superionic conductor,[3] has been widely used to prepare nonlinear optical devices,[4] photochargeable secondary batteries,[5] and multipurpose ion-selective electrodes.[6]

For the above-mentioned applications, a variety of techniques have been developed to prepare silver chalcogenides with controllable microstructure, morphology and particle size. Recently, special attention has been paid to shape control of nanocrystals, which is becoming a challenging problem for the synthesis of nanoscale materials.[7] In particular, fractal structures have attracted much attention in the past two decades.[8] Fractals are generally observed in non-equilibrium growth phenomena, therefore they can provide a natural framework for the study of disordered systems. Examples are many and varied, ranging from the growth of a snowflake to the aggregation of a soot particle, from oil recovery by fluid injection to solidification of metals, and from the formation of a coral reef to cell differentiation during embryonic development. Dendrites, as a kind of fractal structure, have received intensive interest in recent years. There are a variety of methods to be used for preparing dendritic supramolecular nanostructures.[9]

Of the various methods available to prepare nanoscale materials, a template method in which the desired materials are encapsulated into the channels or pores of a host has a number of interesting and useful features for the preparation of nanostructures, since the size and shape of the desired materials can be easily adjusted using a well-defined template matrix.[10] Many templates have emerged, such as carbon nanotubes,[11] porous anodic alumina,[12] "track-etch" polycarbonate membranes,[13] micelles,[14] block copolymers,[15] mesoporous silica,[16] and hybrid organic–inorganic mesoporous material.[17]

As described elsewhere,[18] Raney nickel can be obtained by leaching the aluminium from Ni–Al alloy in NaOH solution. Aluminium is dissolved from the material in alkaline solution and a porous structure is obtained. The residue after leaching of the Al component consists mainly of Ni in a highly dispersed state (surface areas of 50 to 120 $m^2\ g^{-1}$),[18] thus Raney nickel is also named skeleton nickel. The scanning electron microscopy (SEM) image of Raney nickel can be found in the literature.[19] It indicates that Raney nickel is composed of the pores arranged in a crisscross pattern with a supporting skeleton. Raney nickel, as a porous material, has found widespread applications in the field of the hydrogenation of organic compounds[19] and especially as an anode in liquid fuel cells.[20] Theoretically speaking, Raney nickel is attractive as a host framework for the preparation of nanoscale materials in addition to its applications in catalysis. Previously, we have succeeded in synthesizing well-defined palladium and silver dendrites *via* a novel ultrasonic-assisted template-based route, in which Raney nickel was used as the template for the first time.[21] In this work, we extend this route to prepare nanoscale dendrites of silver chalcogenides. To our knowledge, dendrites of silver chalcogenides have not, as yet, been reported.

Experimental

About 3 g of Ni/Al (Ni% $\approx$ 40–50%, weight ratio) alloy was covered with an excess of NaOH solution in a beaker. Then, the reaction product was rinsed several times with distilled water until no further evolution of hydrogen could be observed. The as-prepared Raney nickel was kept immersed in distilled water. Stoichiometric mixtures of analytically pure $AgNO_3$ and S (or Se) powder were put into a 100 mL conical flask containing the above as-obtained Raney nickel, which was then filled with distilled water up to 75% of the total volume. The flask was immersed in a commercial ultrasonic cleaner (WuXi, H-66025, 220 V, 100 W). The whole reaction procedure was performed at room temperature and ambient pressure and lasted for 2 h. Then, the precipitates were filtered, washed with dilute HCl, ethanol and distilled water in sequence, and then dried under vacuum at room temperature for 4 h. Finally, the products were collected for characterization.

X-ray diffraction (XRD) analysis was carried out with a Japan Rigaku D/max-rA X-ray diffractometer with graphite monochromatized Cu Kα radiation (λ = 1.54178 Å). A scanning rate of 0.06° s^{-1} was applied to record the XRD patterns in the 2θ range of 10–70°. In order to obtain information about the composition of the products, X-ray photoelectron spectroscopy (XPS) was performed on an

 DOI: 10.1039/b110249d

ESCALab MKII X-ray photoelectron spectrometer, using Mg Kα X-ray as the excitation source. The binding energies obtained in the XPS analysis were calibrated against the C 1s peak at 284.6 eV. Transmission electron microscopy (TEM) images and selected-area electron diffraction (SAED) patterns were taken on a Hitachi Model H-800 transmission electron microscope with an accelerating voltage of 200 kV. The atomic ratios of the silver chalcogenides were measured on a Seiko Electronics SPD 1200A inductively coupled plasma (ICP) emission analyzer with a pump flow of 1.85 mL min^{-1} and an auxiliary gas (Ar 99.99%) flow rate of 0.5 L min^{-1}. UV-Vis absorption spectra were taken on a JGNA Specord 200 PC UV-Vis spectrophotometer when ethanol was used as a reference.

Results and discussion

The XRD patterns of the products are shown in Fig. 1 for Ag_2S (a) and Ag_2Se (b). In Fig. 1a, all the reflections could be indexed to the monoclinic Ag_2S phase with as-calculated lattice constants $a = 4.191$ Å, $b = 6.872$ Å, $c = 7.811$ Å, in good agreement with the reported data for Ag_2S (JCPDS Card File, 14-72). On the other hand, the orthorhombic Ag_2Se phase was obtained in our experiment with as-calculated lattice constants $a = 4.302$ Å, $b = 6.972$ Å, $c = 7.741$ Å, which accord well with the literature values for Ag_2Se (JCPDS Card File, 24-1041). In both XRD patterns, no impurity peaks were detected in the experimental range. Further evidence for the purity and composition of the products was obtained by XPS measurements. For Ag_2S, the results in the spectra show that the binding energies of Ag $3d_{5/2}$ and S 2p are 368.1 and 161.3 eV, respectively, which are consistent with the reported data of Ag_2S.[22] For Ag_2Se, the two strong peaks at 367.9 and 53.7 eV corresponding to Ag $3d_{5/2}$ and Se $3d_{5/2}$ binding energies, respectively, are consistent with the reported data of Ag_2Se.[22] In order to avoid lengthiness of this paper, XPS spectra of only Ag_2S are shown in Fig. 2. Both XRD and XPS analyses show that the products are pure (without contamination) within the limits of instrumental error. The atomic ratio of Ag_2E obtained from the integrated areas of Ag 3d and S 2p (or Se 3d) peaks is 1.97 : 1 (or 2.04 : 1), which is close to that obtained from ICP elemental analysis of $Ag_{1.98}S$ (or $Ag_{2.02}Se$).

Typical TEM images of the products are illustrated in Fig. 3 for Ag_2S (a) and Ag_2Se (b), indicating that the two samples are well-defined nanoscale dendrites. Furthermore, the highly

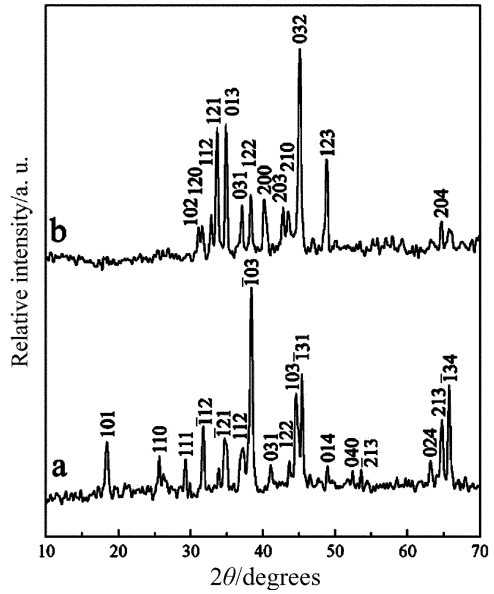

Fig. 1 XRD patterns of (a) Ag_2S and (b) Ag_2Se dendrites.

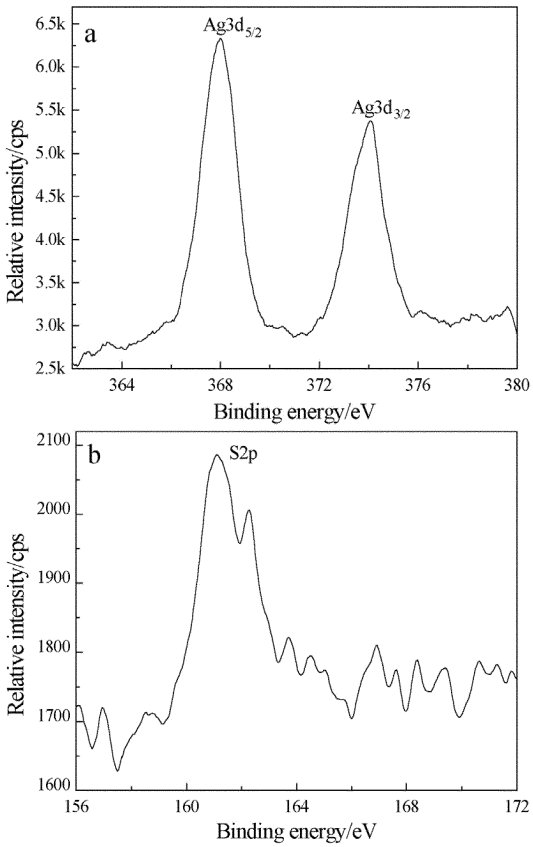

Fig. 2 XPS analysis for Ag_2S dendrites: (a) Ag 3d spectrum, (b) S 2p spectrum.

crystalline nature of the samples was confirmed by SAED measurements made on these dendrites. The SAED patterns are shown in the corresponding insets. The appearance of diffraction dots indicates that the two products are comprised of single crystalline domains.

In our experiment, Ag^+ firstly diffuses into the pores of Raney nickel under the action of the ultrasonic wave. Then, Ag^+ in the pore is reduced by Raney nickel to metallic Ag, which immediately reacts with S (or Se) to form Ag_2S (or Ag_2Se) due to the high reactivity of the renascent Ag. At the same time, interspaces in the skeleton of Raney nickel form due to the reaction of Raney nickel with Ag^+. Later, Ag^+ most certainly re-diffuses into these interspaces and is again reduced by Raney nickel to form silver, which is also transformed into silver chalcogenides. This process lasts until Ag^+ disappears completely. Thus, silver chalcogenides that are formed in the pores become the trunk of dendrite and silver chalcogenides

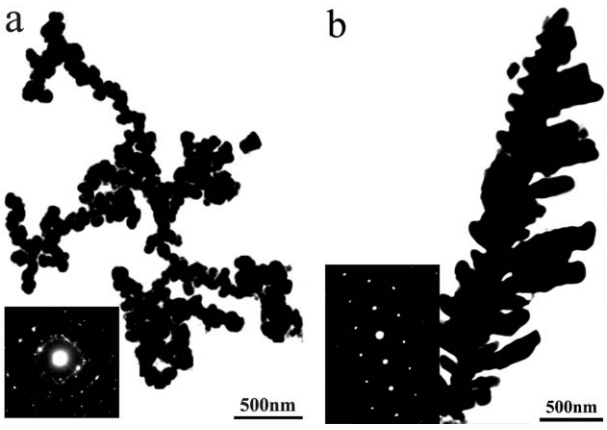

Fig. 3 TEM images of (a) Ag_2S and (b) Ag_2Se dendrites. SAED patterns recorded on dendrites are shown in the corresponding insets.

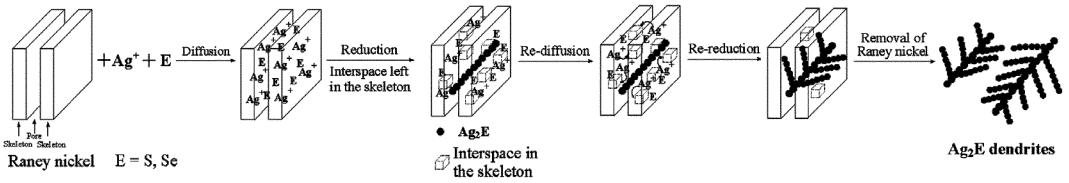

Scheme 1 Schematic illustration of the growth process of Ag_2E dendrites.

that form in the interspaces become the branches. Finally, well-defined nanoscale dendrites of silver chalcogenides appear after the removal of unreacted Raney nickel by HCl solution. The whole process is illustrated diagrammatically in Scheme 1, in which the pore structure of Raney nickel is represented by two end-open flat structures for simplification.[23] From this Scheme, we can see that it is the formation of the interspaces in the skeleton that leads to the fractal of silver chalcogenides. The formation of the interspaces indicates that Raney nickel indeed plays an important role as the reducing agent in addition to the template for the growth of dendrites.

It is found that the template and the ultrasonic wave play important roles in the formation of well-defined nanoscale dendrites. When this reaction was carried out without Raney nickel as the template and reducing agent, only irregular nanoparticles were obtained using ethanol or methanol as the reductant and keeping other reaction conditions unchanged. A TEM image of thus-formed irregular nanoparticles of silver chalcogenides is shown in Fig. 4a. On the other hand, ill-defined dendrites, the TEM image of which is shown in Fig. 4b, were prepared without the action of an ultrasonic wave. Without the template, nanoparticles of silver chalcogenides instead of dendrites were certainly obtained. As for no use of an ultrasonic wave, ill-defined dendrites were prepared, since Ag^+ could not diffuse into the pores of Raney nickel fully. It is well known that an ultrasonic wave can accelerate Ag^+ to diffuse into the pores of Raney nickel,[24] leading to the formation of well-defined nanoscale dendrites.

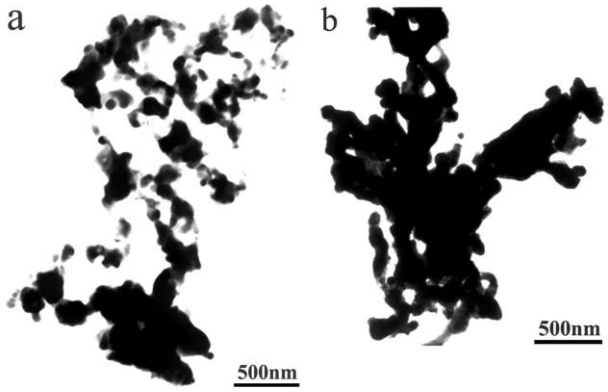

Fig. 4 TEM images of (a) nanoparticles and (b) ill-defined dendrites of silver chalcogenides.

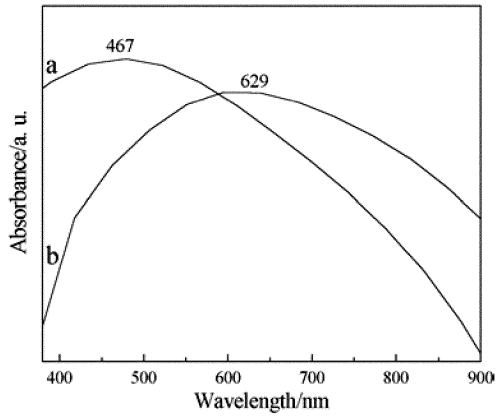

Fig. 5 UV-Vis spectra of (a) Ag_2S and (b) Ag_2Se dendrites.

UV-Vis spectra of the products, which were obtained from the supernates of Ag_2E powders redispersed in ethanol solution, are shown in Fig. 5. The two spectra are broadened, and the absorption maxima of Ag_2S and Ag_2Se are 467 and 629 nm respectively. Compared with the literature values of the band gap of bulk silver chalcogenides,[25] the apparent large blue shift of the observed absorption clearly indicates that the as-prepared Ag_2S and Ag_2Se nanoscale dendrites are within the quantum confinement regime.

Conclusions

In summary, well-defined nanoscale Ag_2S and Ag_2Se dendrites with quantum confined effect have been successfully synthesized *via* a template-based method at room temperature and ambient pressure. It is found that the template and ultrasonic wave play important roles in the formation of well-defined dendrites of silver chalcogenides. This interesting morphology of silver chalcogenides may have potential use in the semiconductor industry.

Acknowledgement

Financial support from the Chinese National Science Foundation of Natural Science Research and the Chinese Ministry of Education is gratefully acknowledged.

References

1 (*a*) N. N. Greenwood and E. A. Earnshaw, *Chemistry of the Elements*, Pergamon, Oxford, 1990, p. 1403; (*b*) G. Nickless, *Inorganic Chemistry of Sulphur*, Elsevier, London, 1968, p. 670.
2 G. L. DeRycke and F. Henderickx, European Patent Application No. 89202613, 9, 1990.
3 (*a*) F. Shimojo and H. Okazaki, *J. Phys. Soc. Jpn.*, 1993, **62**, 179; (*b*) K. Honma and K. Iida, *J. Phys. Soc. Jpn.*, 1987, **56**, 1828; (*c*) T. Sakuma, K. Iida, K. Honma and H. Okazaki, *J. Phys. Soc. Jpn.*, 1977, **43**, 538.
4 K. L. Lewis, A. M. Pitt, T. Wyatt-Davies and J. R. Milward, *Mater. Res. Soc. Symp. Proc.*, 1994, **374**, 105.
5 T. Akoto, Y. Hasuda, M. Ishizawa and T. Horie, *Jpn. Kokai Tokyo Koho* JP 04. 171, 681.
6 B. Nesie and M. S. Jovanovic, *J. Serb. Chem. Soc.*, 1991, **56**, 353.
7 (*a*) X. G. Peng, L. Manna, W. D. Yang, J. Wickham, E. Scher, A. Kadavanich and A. P. Alivisatos, *Nature*, 2000, **404**, 59; (*b*) V. F. Puntes, K. M. Krishnan and A. P. Alivisatos, *Science*, 2001, **291**, 2115.
8 (*a*) L. M. Sander, *Nature*, 1986, **322**, 789; (*b*) J. Nittmann and H. E. Stanley, *Nature*, 1986, **321**, 663; E. Ben-Jacob and P. Garik, *Nature*, 1990, **343**, 523; (*c*) S. Z. Wang and H. W. Xin, *J. Phys. Chem. B*, 2000, **104**, 5681.
9 (*a*) S. T. Selvan, *Chem. Commun.*, 1998, 351; (*b*) Y. Zhou, S. H. Yu, C. Y. Wang, X. G. Li, Y. R. Zhu and Z. Y. Chen, *Adv. Mater.*, 1999, **11**, 850.
10 (*a*) C. R. Martin, *Chem. Mater.*, 1996, **8**, 1739; (*b*) C. Schönenberger, B. M. I. Van der Zande, L. G. J. Fokkink, M. Henny, C. Schmid, M. Krüger, A. Bachtold, R. Huber, H. Birk and U. Staufer, *J. Phys. Chem. B*, 1997, **101**, 5497; (*c*) L. Sun, P. C. Searson and C. L. Chien, *Appl. Phys. Lett.*, 1999, **74**, 2803; (*d*) S. Shingubara, O. Okino, Y. Sayama, H. Sakaue and

T. Takahagi, *Solid-State Electron.*, 1999, **43**, 1143; (*e*) S. A. Sapp, B. B. Lakshmi and C. R. Martin, *Adv. Mater.*, 1999, **11**, 402.
11 (*a*) H. J. Dai, E. W. Wong, Y. Z. Lu, S. S. Fan and C. M. Lieber, *Nature*, 1995, **375**, 769; (*b*) W. Q. Han, S. S. Fan, Q. Q. Li and Y. D. Hu, *Science*, 1997, **277**, 1287; (*c*) B. K. Pradhan, T. Kyotani and A. Tomita, *Chem. Commun.*, 1999, 1317.
12 (*a*) C. K. Preston and M. Moskovits, *J. Phys. Chem.*, 1993, **97**, 8495; (*b*) D. Moutkevitch, T. Bigioni, M. Moskovits and J. M. Xu, *J. Phys. Chem.*, 1996, **100**, 14037; (*c*) Z. Zhang, J. Y. Ying and M. S. Dresselhaus, *J. Mater. Res.*, 1998, **13**, 1745.
13 C. R. Martin, *Science*, 1994, **266**, 1961.
14 R. Schöllhorn, *Chem. Mater.*, 1996, **8**, 1747.
15 H. L. Frisch and J. E. Mark, *Chem. Mater.*, 1996, **8**, 1735.
16 (*a*) M. J. MacLachlan, P. Aroca, N. Coombs, I. Manners and G. A. Ozin, *Adv. Mater.*, 1998, **10**, 144; (*b*) M. H. Huang, A. Choudrey and P. D. Yang, *Chem. Commun.*, 2000, 1063; (*c*) H. J. Shin, R. Ryoo, Z. Liu and O. Terasaki, *J. Am. Chem. Soc.*, 2001, **123**, 1246; (*d*) K. B. Lee, S. M. Lee and J. Cheon, *Adv. Mater.*, 2001, **13**, 517; (*e*) H. Kang, Y. W. Jun, J. I. Park, K. B. Lee and J. Cheon, *Chem. Mater.*, 2000, **12**, 3530; (*f*) H. Parala, H. Winkler, M. Kolbe, A. Wohlfart, R. A. Fisher, R. Schmechel and H. von Seggern, *Adv. Mater.*, 2000, **12**, 1050; (*g*) Z. Liu, Y. Sakamoto, T. Ohsuna, K. Hiraga, O. Terasaki, C. H. Ko, H. J. Shin and R. Ryoo, *Angew. Chem., Int. Ed. Engl.*, 2000, **39**, 3107.
17 A. Fukuoka, Y. Sakamoto, S. Guan, S. Inagaki, N. Sugimoto, Y. Fukushima, K. Hirahara, S. Iijima and M. Ichikawa, *J. Am. Chem. Soc.*, 2001, **123**, 3373.
18 J. Rothe, J. Hormes, C. Schild and B. Pennemann, *J. Catal.*, 2000, **191**, 294.
19 J. P. Mikkola, H. Vainio, T. Salmi, R. Sjöholm, T. Ollonqvist and J. Väyrynen, *Appl. Catal. A: Gen.*, 2000, **196**, 143.
20 E. W. Justi and A. W. Winsel, *J. Electrochem. Soc.*, 1961, **108**, 1073.
21 J. P. Xiao, Y. Xie, R. Tang, M. Chen and X. B. Tian, *Adv. Mater.*, 2001, **13**, 1887.
22 J. F. Moulder, W. F. Stickle, P. E. Sobol and K. D. Bomben, *Handbook of X-ray Photoelectron Spectroscopy*, ed. J. Chastain, Perkin-Elmer Corp., Eden Prairie, MN, 1992.
23 Catalysis Group, Department of Chemistry, Jilin University, *Basis of Catalysis*, Science Press, Beijing, 1977, p. 63 (in Chinese).
24 (*a*) K. Chatakondu, M. L. H. Green, M. E. Thompson and K. S. Suslick, *J. Chem. Soc., Chem. Commun.*, 1987, 900; (*b*) K. S. Suslick and G. J. Price, *Annu. Res. Mater. Sci.*, 1999, **29**, 295.
25 (*a*) M. C. Brelle, J. Z. Zhang, L. Nguyen and R. K. Mehra, *J. Phys. Chem. A*, 1999, **103**, 10194; (*b*) M. von der Oster, *Landolt-Bornstein*, 1982, **172**, 156.